Hindawi
Advances in Civil Engineering
Volume 2023, Article ID 8829409, 10 pages
https://doi.org/10.1155/2023/8829409

Research Article

Surface Properties of Concrete and Bonding Strength of Pine Resin-Based Adhesives to Concrete Surfaces

Se-Eon Park,[1] **Jeong-Il Choi**,[2] **Sungho Lee**,[3] **Eung-Sam Kim**,[4] **Bong-Kee Lee**,[5] **and Bang Yeon Lee**[6]

[1]*Department of Architecture and Civil Engineering, Chonnam National University, Gwangju 61186, Republic of Korea*
[2]*Biohousing Research Center, Chonnam National University, Gwangju 61186, Republic of Korea*
[3]*Department of Biological Sciences, Chonnam National University, Gwangju 61186, Republic of Korea*
[4]*Department of Biological Sciences, Research Center of Ecomimetics, Chonnam National University, Gwangju 61186, Republic of Korea*
[5]*School of Mechanical Engineering, Chonnam National University, Gwangju 61186, Republic of Korea*
[6]*School of Architecture, Chonnam National University, Gwangju 61186, Republic of Korea*

Correspondence should be addressed to Bang Yeon Lee; bylee@jnu.ac.kr

Received 6 December 2022; Revised 16 January 2023; Accepted 28 January 2023; Published 8 February 2023

Academic Editor: Peng Zhang

This article reports a quantitative investigation of the surface characteristics of normal concrete manufactured with different types of formworks and bonding strength between pine resin-based adhesives and concrete surfaces. Three types of formworks and adhesives with different ratios of pine resin to wax were prepared. Scanning electron microscopy, energy-dispersiveX-ray spectroscopy, white-light scanning interferometry, and electrophoretic light scattering were utilized for the surface characterization of concrete, and a bonding test was performed. Test results showed that the surface roughness of concrete was significantly influenced by the type of formwork; all techniques including visual observation provided similar results. On the contrary, chemical compositions and electrical characteristics were not influenced by the type of formwork. Bonding test results showed that bonding strength increased as the ratio of wax increased and the degree of the concrete surface roughness increased. The results of this study indicate the feasibility of pine resin-based adhesives for concrete structures as green construction materials.

1. Introduction

According to the 2021 report card for America's infrastructure released by the American Society of Civil Engineers (ASCEs), the average grade of the 17 categorized types of infrastructure was C-, slightly higher than the grade (D) in 1998 when these evaluations began. However, eleven categories were still graded D [1]. Among the most important parts of this evaluation are accurate investigations and reasonable assessments of structures [2]. Studies of various sensors and evaluation and diagnosis systems along with proper assessment procedures are actively conducted for accurate evaluations and assessments of structures [3–10]. The investigation of concrete structures is performed by permanently attaching measurement devices or sensors to concrete surfaces or by employing noncontact methods. When a measurement device or sensor is attached to concrete, the adhesive force depends on the type of adhesive material and the concrete surface characteristics.

Materials used for adhesion to the concrete are mostly synthetic organic compounds comprising chains of carbon linked to hydrogen, oxygen, etc. Epoxy resin is a typical synthetic material used with concrete for coating, repair, sealing, wearing surface, grouting, etc. [11].

Studies have been conducted to evaluate concrete surface adhesion characteristics under various conditions and environments and to develop new adhesive materials [12–15]. Previous studies reported that adhesion properties between adhesives and concrete surfaces are influenced by types of adhesives, surface properties of concrete, surface treatment

of concrete, and environmental conditions. Horgnies et al. performed peel tests to investigate the adhesion between polyurea-based protective coating and concrete; Fourier transformed infra-red (FT-IR) spectroscopy was adopted to characterize fracture loci during adhesion [13]. Test results showed that humid curing conditions and long-term aging significantly decrease adhesion by 50% and 80%, respectively, mainly due to the closure of pores, the weak interface of plate-shaped portlandite, efflorescence, and carbonation. It was demonstrated that adhesion between polyurea-based coating materials and concrete is achieved by mechanical anchorage at the concrete surface. Krzywiński and Sadowski prepared a total of seventeen types of concrete with different surface textures by grooving, imprinting, patch grabbing, and brushing; they then measured the pull-off strength of the epoxy resin coatings [12]. From their test results, it was found that the pull-off strength was highest (pull-off strength: 2.00 MPa) when the surface was prepared by imprinting. Ye et al. investigated the interfacial bonding strength of geopolymer and wood (spruce and beech) composites [14]. Test results showed that the bonding strength increased with the embedded depth of the wood up to 25 mm. The interfacial bonding strength values for spruce and beech were 0.8 MPa and 0.6 MPa, respectively, when the embedded depth was 25 mm. It was also observed that a wood surface roughened by sanding with 60-grit sandpaper induced higher bonding strength than strong mechanical interlocking at the interface.

As described previously, fossil-fuel-based adhesives such as epoxy, acrylic, and polyurethane are widely used in concrete construction processes. Although research on bio-based adhesives for concrete construction is required due to the social demand for independence from fossil fuels, no significant work on bio-based adhesives for concrete has been reported in the literature. This research aims to address this knowledge gap.

The objective of the current study is to investigate quantitatively the physical and chemical properties of concrete surfaces according to the type of formwork and the bonding properties between concrete and pine resin-based adhesives.

2. Materials and Methods

2.1. Materials. Table 1 lists the materials and mixture proportion of concrete used in the present study. The main parameters influencing the concrete properties such as water-to-cement ratio and aggregate ratio were determined from the normal mixture proportions of concrete used at construction sites. Ordinary type I Portland cement was used as a binder, along with tap water. Jumunjin standard sand and gravel with a maximum size of 13 mm were used as fine aggregate and coarse aggregate, respectively. A liquid polycarbonate-based superplasticizer was used to ensure proper rheological properties of concrete. To minimize large pores during the mixing process, an antifoamer based on mineral substances, without silicone, was used. After mixing the components, three cylindrical specimens with dimensions of $\phi 100\,\text{mm} \times 200\,\text{mm}$ were manufactured for the compressive strength tests; three-panel specimens with dimensions of $200\,\text{mm} \times 200\,\text{mm} \times 40\,\text{mm}$ were manufactured for the adhesion tests. Plastic sheets were placed on tops of molds to minimize moisture evaporation; then, samples were cured in a room with a controlled temperature of $(23 \pm 3)\ ^\circ\text{C}$ for 1 day. All specimens were removed from molds and cured under identical conditions until the age of 28 days. The compressive strength was measured according to ASTM C39/C39M; the average compressive strength of concrete was 46.3 MPa. For the adhesion tests, panel specimens were cut into small pieces with dimensions of $40\,\text{mm} \times 40\,\text{mm} \times 40\,\text{mm}$.

Three different types of wood molds for formwork were used in the present study. The surfaces of these molds are shown in Figure 1. The FN and FC formworks were a general plywood formwork and a surface-coated plywood formwork, respectively, both of which are commonly used at construction sites. The FS formwork was a mold prepared by attaching sandpaper to a general plywood formwork to simulate either deterioration of the concrete surface or an artificially roughened surface. P100 sandpaper consisting of aluminum oxide particles with mean particle diameters of 162 μm was used to roughen the SF formwork. Identical IDs were used for concrete specimens.

Table 2 lists the ratios of pine resin to wax for the adhesives investigated in the present study. The specimen IDs are shown in the form of "F*a*-P*b*W*c*," where F, P, and W denote the formwork, pine resin, and wax, respectively. In addition, *a* and *b*/*c* represent concrete specimens manufactured using different types of formwork and with the two pine resin/wax ratios. The melting point of the adhesive pine resin ranged from 70°C to 80°C. When molten pine resin is cured at room temperature to solidify it, it can become brittle due to rapid heat loss. Wax is known to have adhesive properties; its melting point is on average 62°C but depends on the mixtures of components. Since wax has a lower melting point than pine resin, it has a longer curing time, making it more malleable than pine resin. The mixed wax used in this work consisted of 60% nonpurified beeswax, 30% paraffin, and 10% ceresin.

2.2. Test Methods. To evaluate the surface characteristics of concrete, concrete specimen surfaces manufactured according to the type of formwork were visually observed; images were obtained using a digital camera. Scanning electron microscopy (SEM) and energy-dispersiveX-ray spectroscopy (EDS) analyses were used to observe the microstructures and chemical compositions of specimens. The accelerating voltage of the EDS configuration was 15 kV; SEM/EDS investigation was performed only using the secondary electron imaging mode. Samples were prepared by cutting off pieces of the surface with sizes of about $1 \times 1 \times 1\,\text{cm}^3$; the prepared samples were held under vacuum for 3 days and coated with platinum.

To quantitatively measure the roughness of the concrete surface, white-light scanning interferometry (WSI), which irradiates visual light onto the surface and measures the wavelength of reflected light to identify the surface shape,

Table 1: Mixture proportions (proportion by weight).

Cement	Water	Fine aggregate	Coarse aggregate	Superplasticizer	Antifoamer
1	0.41	2.06	2.42	0.007	0.001

(a) (b) (c)

Figure 1: Types of formworks: (a) FN, (b) FC, and (c) FS.

Table 2: Adhesive materials.

	Pine resin	Wax
P1W9	0.1	0.9
P3W7	0.3	0.7
P5W5	0.5	0.5

was employed. Specimens with sizes similar to those used in the SEM/EDS investigation were coated with gold (Ag) to ensure surface reflection of visual light. Three specimens for each type of concrete manufactured with the different types of formwork were prepared. After measurements, surfaces were imaged in 2D and 3D using a software program, and the surface roughness was quantitatively represented by three parameters. The arithmetic mean roughness (R_a) indicates the average of the absolute values between the average height (or depth) and the height at a certain position. Therefore, high R_a in general means a rough object surface. R_a is calculated using the following equation:

$$R_a = \frac{1}{A}\int_0^A |r(x,y)|\mathrm{d}A, \tag{1}$$

where $r(x,y)$ is the difference between the average height and height at position x, y and A is the measurement area.

R_q is the root mean square average roughness, calculated using the following equation:

$$R_q = \sqrt{\frac{1}{A}\int_0^A r^2(x,y)\mathrm{d}A}. \tag{2}$$

R_t is the difference between the maximum ($h_{\max}$) and minimum ($h_{\min}$) heights, as calculated using equation (3). Although R_t does not indicate the average roughness, it can be a feature of the surface roughness.

$$R_t = \left|h_{\max} - h_{\min}\right|. \tag{3}$$

The zeta potential (ζ) was measured to understand the electrical characteristics of the concrete surfaces. Samples in powder form were acquired using a diamond grinder on the specimen surfaces. Subsequently, a zeta potential analyzer using electrophoretic light scattering and having a measurement range of 0.1 nm to 10 μm and a zeta potential from −200 mV to 200 mV was used to measure the zeta potential. Distilled water was used as an aqueous solution for zeta potential measurement. Six samples from each of the concrete specimens with different types of formwork were used in the measurement. The zeta potentials of the samples were calculated using the Helmholtz–Smoluchowski equation [16], based on the speed of the particles measured in a constant electric field. The Helmholtz–Smoluchowski equation is shown in the following equation:

$$\zeta = \eta U_0 \varepsilon^{-1} \varepsilon_0^{-1}, \tag{4}$$

where ζ denotes the zeta potential, η the viscosity of the aqueous solution, U_0 the electrophoretic mobility of the concrete particles, and ε and ε_0 the dielectric constants of the aqueous solution and vacuum, respectively.

Figure 2 shows the adhesion test setup. Two small specimens with dimensions of 40 mm × 40 mm × 40 mm were manufactured using the same types of formworks that were used for the adhesion tests. Transparent plastic films with holes with a diameter of 15 mm were attached to the sides of one of two small specimens to maintain identical adhesion areas for each test (Figure 2(a)). It should be mentioned that adhesion between the concrete surface and the transparency film was negligible. Using epoxy, jigs to fix specimens to the test machine were attached to the other sides of the two small specimens (Figure 2(b)). Using a heating mantle, pine resin flakes, and wax were heated above 100°C until they became liquid; this took approximately 1 min. The liquid adhesive was poured on the top surfaces of the specimens; then, the other specimens with transparency films were attached within 10 s. Each specimen was tested after 1 hour. Adhesion tests were performed using a universal testing machine with a capacity of 20 kN. The tensile load was applied by displacement control with a loading speed of 0.4 mm/min. The load was measured via a load cell attached to the machine.

3. Results and Discussion

3.1. Visual Inspection of Concrete Surfaces. Figure 3 provides representative digital camera photos of the concrete surfaces according to the type of formwork. As expected, the concrete surface manufactured using the FS formwork was the roughest of the three. The FC specimen showed a smoother surface.

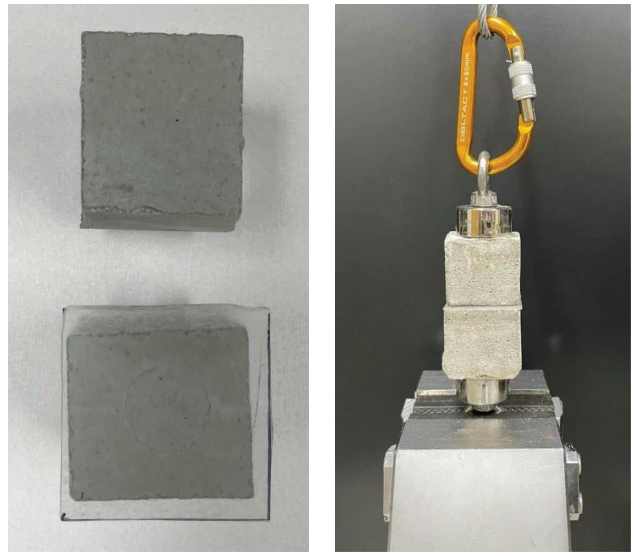

(a) (b)

Figure 2: Adhesion test: (a) specimens and (b) test setup.

3.2. Microstructures and Chemical Compositions of Concrete Surfaces. Figure 4 shows representative SEM images of concrete surfaces according to the type of formwork. Under visual observation, the FN specimen showed a surface pattern similar to that of the plywood formwork; wave-pattern bumps were observed at ×400 magnification. EDS mapping showed evenly distributed Ca and Si elements, the main hydration products, which indirectly indicate the degree of surface roughness. The FC specimen showed a surface smoother than that of the FN specimen at magnifications of both ×40 and ×400. Furthermore, EDS mapping of the Ca and Si elements of the FC specimen showed a distribution more homogenous than that of the FN specimen. In images taken at magnifications of ×40 and ×400, the FS specimen showed the biggest bumps and a rough surface throughout. EDS mapping of Ca and Si elements of FS showed that these elements were less homogenous than they were in the other specimens. Table 3 lists the chemical compositions of the surfaces of the three specimens. No particular trend was observed; however, the most commonly detected components were Ca and Si elements, which are included in the C-S-H gel, the major hydration product.

Figure 5 shows representative 2D and 3D images of the surfaces of individual specimens; both 2D and 3D images indicate that the overall height difference on the surface and the number of micropores in the FC specimen were smaller than those in the FN specimen. On the other hand, the overall height difference on the surface of the FS specimen was greater than that of the FN specimen.

Table 4 lists the parameters used to quantitatively represent the surface roughness. FC specimen showed the lowest R_a value and FS specimen showed the highest R_a value. Identical trends in R_q and R_t were also observed. As can be seen in the images in Figure 5, the quantitative roughness of the concrete surface was lowest in the FC specimens prepared from the coated formwork, and highest in the FN specimens made with the artificially roughened formwork.

3.3. Electrical Characteristics of Concrete Surfaces. Table 5 lists the zeta potential, an electrical characteristic, of the concrete surface, according to the type of formwork. Popov et al. measured concrete zeta potential with various aqueous solutions under different conditions; they reported that concrete zeta potential was in a range of +17 mV to −22 mV [17]. The mean zeta potential measured on the three types of concrete surface in this study was −10.30 mV; this falls into the range of concrete zeta potential found in the previous study. Generally, a zeta potential value near 0 indicates that the electric force on the solid surface is close to 0, resulting in particle aggregation. A large absolute value of zeta potential means that particle dispersion in an aqueous solution has stabilized due to high electric force. Nägele reported that when the SiO- particles on the surface of the cement particles, which are negatively charged, are dispersed in water, Ca^{2+} ions adsorb to the particles, making the particles positively charged [18]. In addition, Lee and Lee reported that cured concrete may have different chemical characteristics because different types and amounts of ions are disassociated depending on the zeta potential, affecting the hydration products [19]. The zeta potential measured on the concrete surfaces formed by the different formworks was highest for the FN specimen (−7.91 mV) and lowest for the FC specimen (−11.60 mV). The zeta potential values of the specimens were slightly different, but the differences were not significant and the values were all negative. Therefore, it is presumed that the type of formwork does not have a significant impact on the electrostatic characteristics of the concrete surface, and thus does not significantly influence the hydration products. This is consistent with the chemical

(a) (b) (c)

Figure 3: Visual inspection of three types of concrete surface manufactured by using (a) FN, (b) FC, and (c) FS formworks.

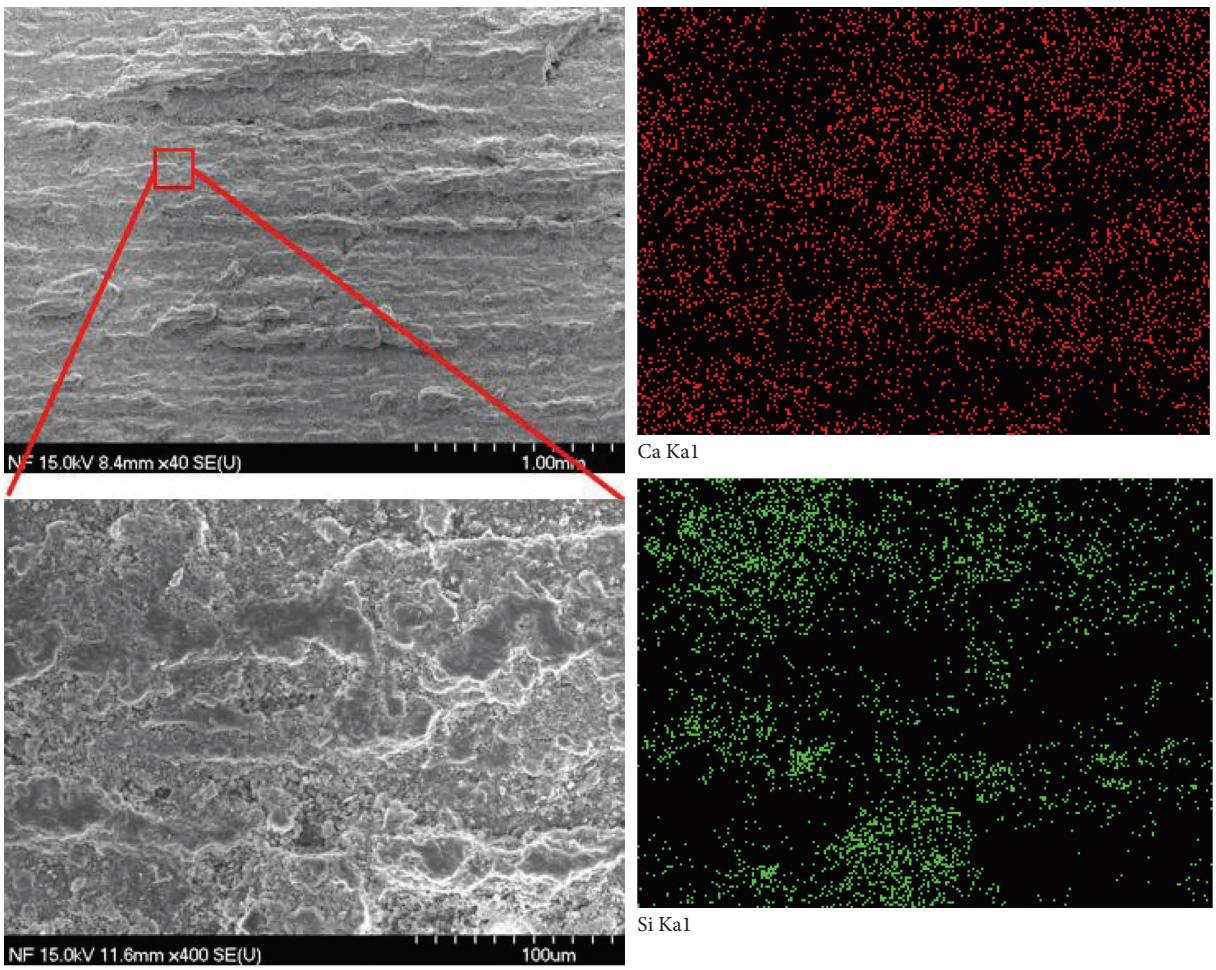

(a)

Figure 4: Continued.

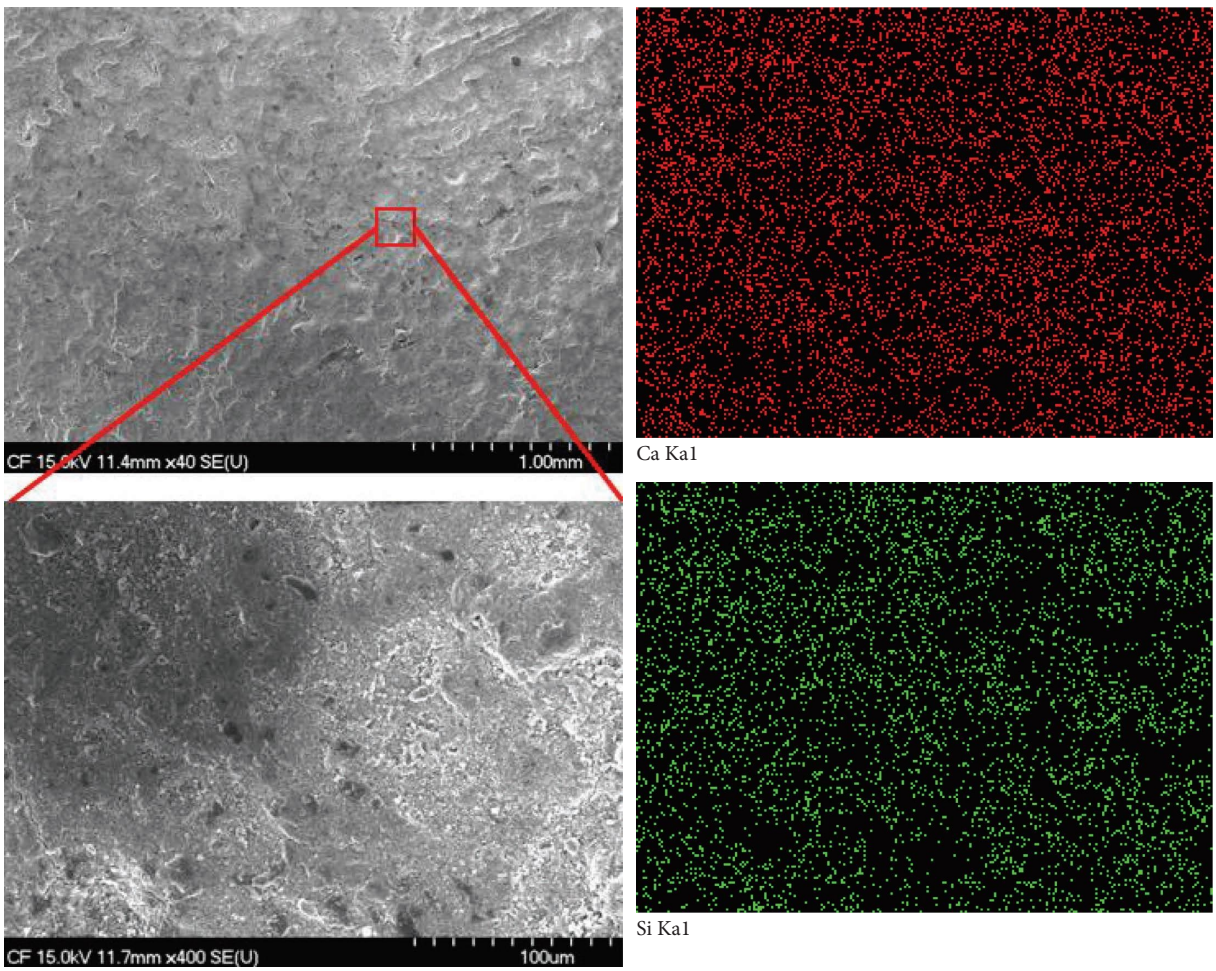

(b)

Figure 4: Continued.

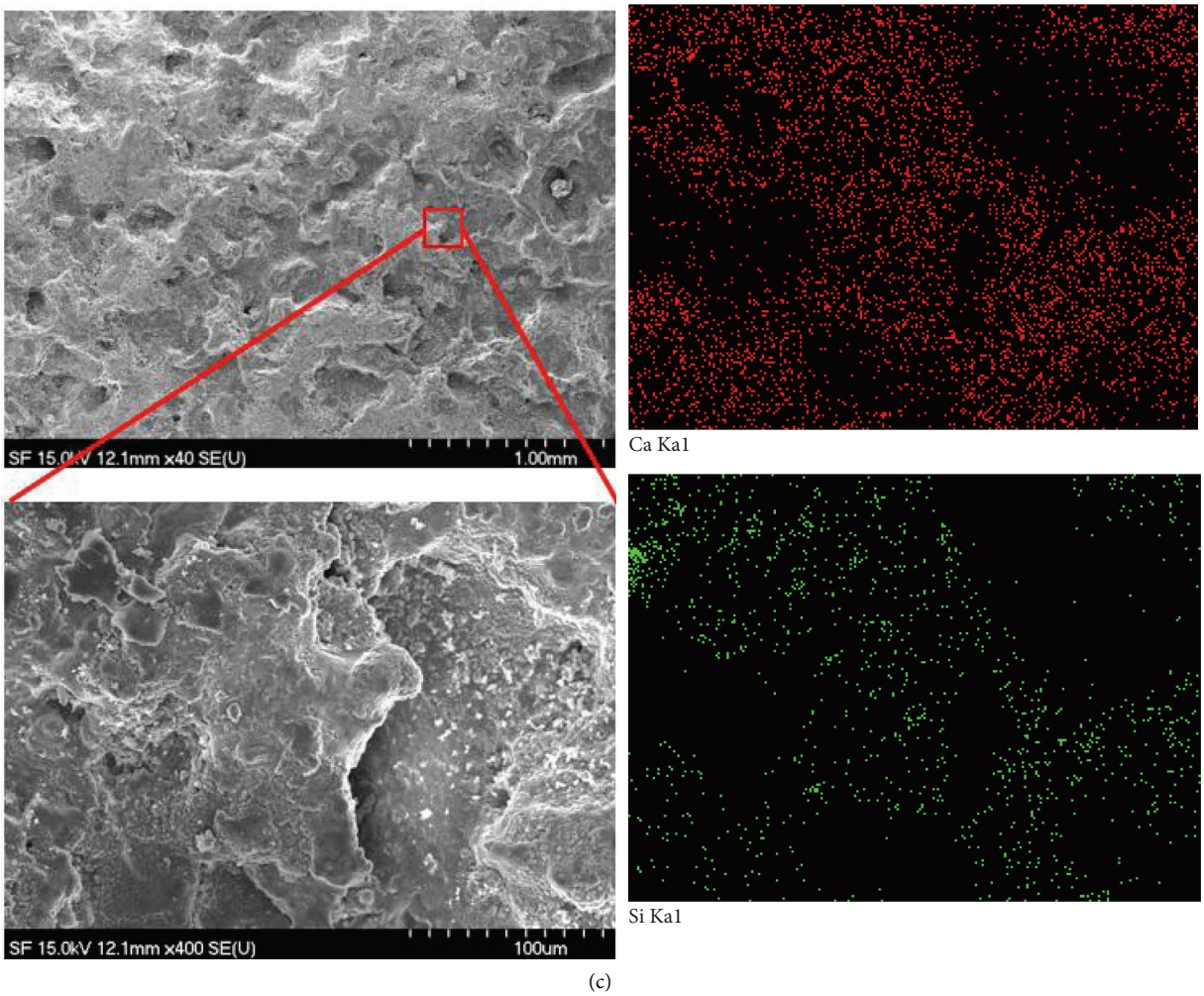

(c)

Figure 4: SEM observation and image mapping of concrete surface: (a) FN, (b) FC, and (c) FS.

Table 3: Chemical compositions of mixtures.

Position	Element with atomic percentage (%)							
	C	O	Na	Mg	Al	Si	S	Ca
FN	2.49	69.81	0.53	0.46	1.36	7.35	0.18	17.82
FC	2.42	66.09	2.14	0.99	2.10	6.69	2.28	17.29
FS	2.17	72.68	0.42	—	0.46	2.75	0.69	20.83

composition analysis results, which showed that the main hydration products were Ca and Si elements, parts of the C-S-H gel.

3.4. Adhesion Properties. Figure 6 shows bond strengths between adhesives with different ratios of pine resin to wax and concrete surface according to the type of formwork. The specimen IDs are shown in the form of "F*a*-P*b*W*c*," wherein F, P, and W denote formwork, pine resin, and wax, respectively. *a* and *b*/*c* denote concrete specimens manufactured using different types of formworks and two pine resin/wax ratios. The values of bonding strength between adhesives and concrete specimens manufactured using coated formwork, widely used in normal construction sites, ranged from 0.99 MPa to 1.41 MPa. It was observed that the bonding strength increased as the amount of wax increased. In more detail, the bonding strength values of P3W7 and P5W5 adhesives were 16.7% and 30.2% lower than that of P1W9 adhesive. This may be attributed to the melting point of the wax, which is lower than that of pine resin, resulting in a large contact area between concrete and an adhesive with high ratio of wax to pine resin due to the longer working time and higher flowability of the adhesive. It is expected that the tensile strength of concrete investigated in this study is 4.6 MPa because this value is approximately 10% of the compressive strength [20]. Therefore, it seems that the bonding strength between the adhesive and concrete surface manufactured using coated formwork ranges from 21% to 30%. Comparing the three specimens FC-P3W7, FN-P3W7,

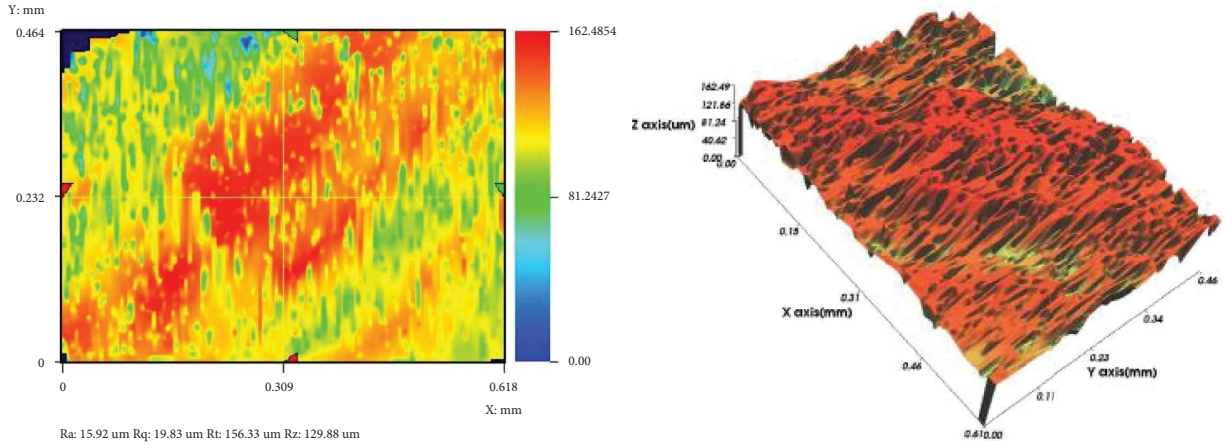

(a)

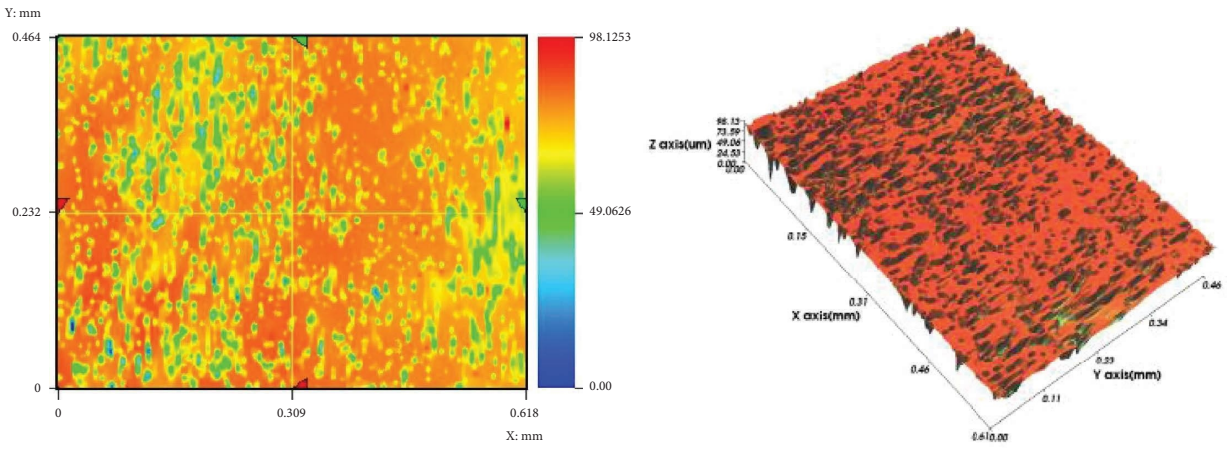

(b)

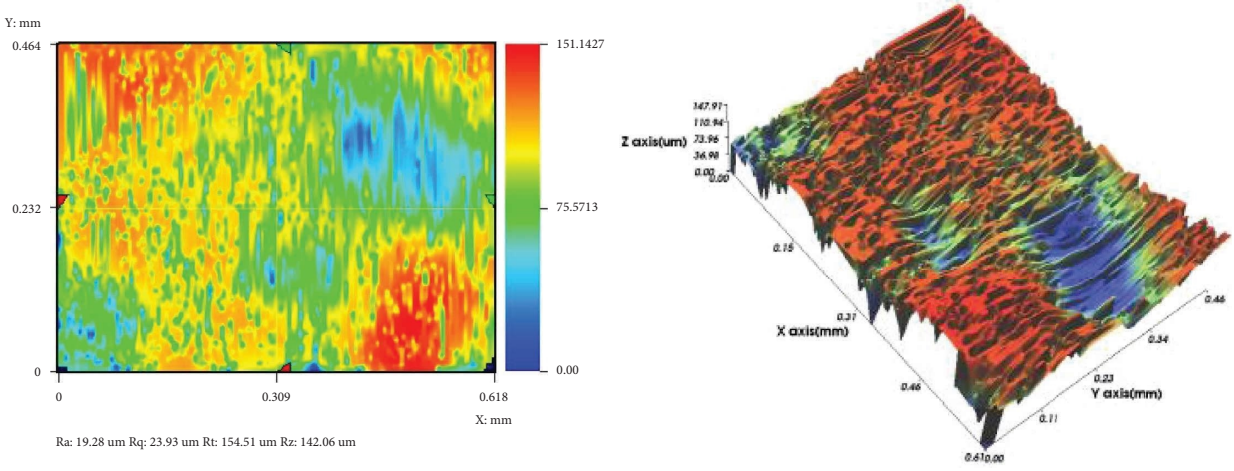

(c)

Figure 5: 2D and 3D profiles of concrete surface: (a) FN, (b) FC, and (c) FS.

Table 4: Surface roughness of concrete (unit: μm).

Specimen	R_a	R_q	R_t
FN	14.14 ± 1.18	17.87 ± 1.12	144.57 ± 14.96
FC	7.83 ± 0.47	10.18 ± 0.53	92.43 ± 6.47
FS	22.46 ± 5.64	27.16 ± 6.19	155.45 ± 7.14

Table 5: Zeta potential (unit: mV).

Specimens	Zeta potential
FN	−9.31 ± 1.27
FC	−11.26 ± 1.16
FS	−10.33 ± 0.78

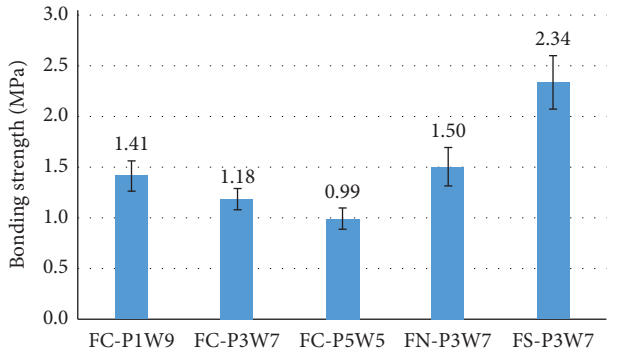

Figure 6: Comparison of bonding strengths of pine resin-based adhesives on concrete surfaces.

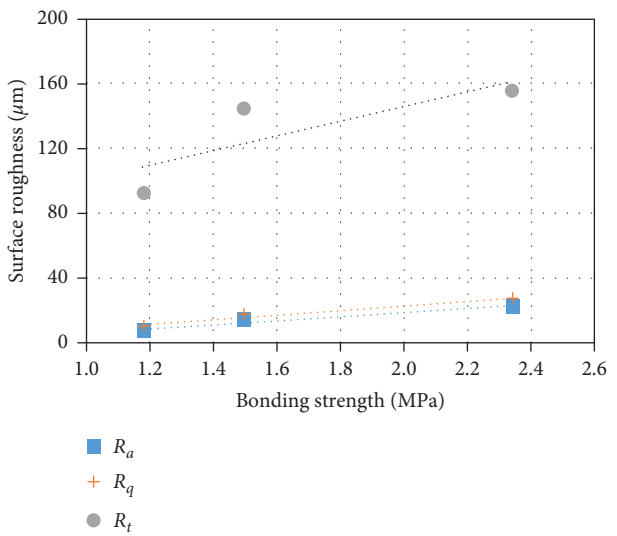

Figure 7: Relationship between the bonding strength and surface roughness of concrete.

and FS-P3W7, for which the same adhesive P3W7 was used, the bonding strength was found to increase as the surface roughness increased. Figure 7 shows the relationship between the bonding strength and the surface roughness of concrete. The correlation coefficient values of FC-P3W7, FN-P3W7, and FS-P3W7 were 0.98, 0.98, and 0.82, respectively, indicating a strong positive correlation between the bonding strength and the surface roughness of concrete. In more detail, the bonding strength values of FN-P3W7 and FS-P3W7 were higher by 27% and 98%, respectively, than that of FC-P3W7. This indicates that the bonding strength of the adhesives investigated in this study may increase when the concrete surface is roughened by surface deterioration.

4. Conclusions

This article investigated the surface properties of concrete manufactured using three types of formwork and looked at the effects of a type of pine resin-based adhesive on bonding strength at the concrete surface. The following conclusions are drawn:

(1) From visual inspection and examination of SEM images, the FC specimen manufactured using coated formwork was found to have a smoother surface than the FN specimen manufactured using a general plywood formwork. The FS specimen manufactured using a formwork with sandpaper to simulate the deterioration of the concrete surface or an artificially roughened surface showed a rougher surface than that of the FN specimen. EDS mapping images of Ca and Si elements also showed results similar to those obtained by visual inspection and SEM observation.

(2) Surface roughness of concrete according to the type of formwork was quantitatively evaluated in terms of three parameters: arithmetic mean roughness, root mean square average roughness, and difference between maximum height and minimum height. FC specimen showed the lowest surface roughness parameters; FS specimen showed the highest surface roughness parameters.

(3) The FN specimen showed the highest (−9.31 mV) zeta potential and the FC specimen showed the lowest (−11.26 mV) zeta potential. The zeta potential values of the specimens were slightly different according to the type of formwork; however, differences were not significant.

(4) The bonding strength between adhesives and concrete manufactured using coated formwork ranged from 0.99 MPa–1.41 MPa; the bonding strength increased as the amount of wax increased. It was also observed that the bonding strength of the adhesives investigated in this study increased as the concrete surface roughness increased.

Data Availability

All datasets generated during this study are available from the corresponding author upon reasonable request.

Conflicts of Interest

The authors declare that they have no conflicts of interest.

Acknowledgments

This work was supported by the Korea Agency for Infrastructure Technology Advancement (KAIA) grant funded by the Ministry of Land, Infrastructure and Transport (Grant no. 22CTAP-C163852-02) and the National Research Foundation of Korea (NRF) grant funded by the Korea Government (MSIT) (Grant nos. 2022R1A2C1007366 and 2022R1A4A1033838).

References

[1] ASCE, *Report Card for America's Infrastructure. 2021*, American Society of Civil Engineers, Reston, VA, USA, 2021.

[2] ISO, *Maintenance and Repair of concrete Structures — Part 2: Assessment of Existing concrete Structures*, International Organization for Standardization, Geneva, Switzerland, 2014.

[3] S. Shahidan, S. S. M. Zuki, and N. Jamaluddin, "Damage grading system for severity assessment on concrete structure," *Case Studies in Construction Materials*, vol. 5, pp. 79–86, 2016.
[4] J. Zhao, T. Hu, R. Zheng, P. Ba, and Q. Zhang, "Design and performance analysis of an ultrasonic system for health monitoring of concrete structure," *Sensors*, vol. 21, no. 19, 2021.
[5] R. Corbally and A. Malekjafarian, "Examining changes in bridge frequency due to damage using the contact-point response of a passing vehicle," *Journal of Structural Integrity and Maintenance*, vol. 6, no. 3, pp. 148–158, 2021.
[6] S. Abdul Kudus, N. Muhamad Bunnori, N. K. Mustaffa, and A. Jamadin, "Investigation on acoustic emission parameters due to fatigue damage of concrete beams with variable notched depth," *International Journal of Concrete Structures and Materials*, vol. 16, no. 1, pp. 29–16, 2022.
[7] X. Chen, Y. Ming, F. Fu, and P. Chen, "Numerical and empirical models for service life assessment of RC structures in marine environment," *International Journal of Concrete Structures and Materials*, vol. 16, no. 1, pp. 11-12, 2022.
[8] S.-Y. Chu, C. J. Kang, M. X. Hu, and L. C. Chang, "Rapid damage assessment of 1/3 scaled-downtwo-story reinforced concrete school building models," *Journal of Structural Integrity and Maintenance*, vol. 7, no. 2, pp. 110–119, 2022.
[9] I. A. Colombani and B. Andrawes, "A study of multi-targetimage-based displacement measurement approach for field testing of bridges," *Journal of Structural Integrity and Maintenance*, vol. 7, no. 4, pp. 207–216, 2022.
[10] R. Wróblewski and B. Stawiski, "Ultrasonic assessment of the concrete residual strength after a real fire exposure," *Buildings*, vol. 10, no. 9, 2020.
[11] N. J. Jin, J. Yeon, I. Seung, and K. S. Yeon, "Effects of curing temperature and hardener type on the mechanical properties of bisphenol F-type epoxy resin concrete," *Construction and Building Materials*, vol. 156, pp. 933–943, 2017.
[12] K. Krzywiński and Ł. Sadowski, "The effect of texturing of the surface of concrete substrate on the pull-off strength of epoxy resin coating," *Coatings*, vol. 9, no. 2, 2019.
[13] M. Horgnies, P. Willieme, and O. Gabet, "Influence of the surface properties of concrete on the adhesion of coating: characterization of the interface by peel test and FT-IR spectroscopy," *Progress in Organic Coatings*, vol. 72, no. 3, pp. 360–379, 2011.
[14] H. Ye, B. Asante, G. Schmidt, A. Krause, Y. Zhang, and Z. Yu, "Interfacial bonding properties of the eco-friendlygeopolymer-wood composites: influences of embedded wood depth, wood surface roughness, and moisture conditions," *Journal of Materials Science*, vol. 56, no. 12, pp. 7420–7433, 2021.
[15] L. Courard, T. Piotrowski, and A. Garbacz, "Near-to-surface properties affecting bond strength in concrete repair," *Cement and Concrete Composites*, vol. 46, pp. 73–80, 2014.
[16] M. V. Smoluchowski, *Handbuch der Elektrizität und des Magnetismus. Band II*, Barth-Verlag, Leipzig, Germany, 1921.
[17] K. Popov, I. Glazkova, S. Myagkov et al., "Zeta-potential of concrete in presence of chelating agents," *Colloids and Surfaces A: Physicochemical and Engineering Aspects*, vol. 299, no. 1-3, pp. 198–202, 2007.
[18] E. Nägele, "The zeta-potential of cement," *Cement and Concrete Research*, vol. 15, no. 3, pp. 453–462, 1985.
[19] B. Lee and J.-S. Lee, "The relationship between the physical properties of mortar mixed with various boron compounds and zeta potential," *Journal of the Korea Concrete Institute*, vol. 33, no. 2, pp. 109–115, 2021.
[20] S. Mindess, J. Young, and D. Darwin, *Concrete*, Pearson Eduction, Upper saddle River, NJ, USA, 2002.